



Published in final edited form as:

Mol Cancer Ther. 2015 October ; 14(10): 2249–2259. doi:10.1158/1535-7163.MCT-15-0429.

Inhibition of wild-type p53-expressing AML by novel small molecule HDM2 inhibitor, CGM097

Ellen Weisberg^{1,*}, Ensar Halilovic^{2,*}, Vesselina G. Cooke², Atsushi Nonami^{1,**}, Tao Ren^{3,***}, Takaomi Sanda^{1,****}, Irene Simkin⁴, Jing Yuan², Brandon Antonakos², Louise Barys⁵, Moriko Ito⁵, Richard Stone¹, Ilene Galinsky¹, Kristen Cowens¹, Erik Nelson^{1,*****}, Martin Sattler¹, Sebastien Jeay⁵, Jens U. Wuerthner⁵, Sean M. McDonough^{1,*****}, Marion Wiesmann^{5,6}, and James D. Griffin^{1,6}

¹Dana Farber Cancer Institute, Harvard Medical School, Boston, MA ²Novartis Institutes of Biomedical Research, Cambridge, MA ³National Screening Laboratory for the Regional Centers of Excellence in Biodefense and Emerging Infectious Diseases Research Harvard Medical School, Boston, MA ⁴Molecular Genetics Core, Boston University School of Medicine, Boston, MA ⁵Novartis Institutes of Biomedical Research, Basel, Switzerland

Abstract

The tumor suppressor, p53, is a key regulator of apoptosis and functions upstream in the apoptotic cascade by both indirectly and directly regulating Bcl-2 family proteins. In cells expressing wild-type (wt) p53, the HDM2 protein binds to p53 and blocks its activity. Inhibition of HDM2:p53 interaction activates p53 and causes apoptosis or cell cycle arrest. Here, we investigated the ability of the novel HDM2 inhibitor, CGM097, to potently and selectively kill wt p53-expressing AML cells. The anti-leukemic effects of CGM097 were studied using cell-based proliferation assays (human AML cell lines, primary AML patient cells and normal bone marrow samples), apoptosis and cell cycle assays, ELISA, immunoblotting, and an AML patient-derived *in vivo* mouse model. CGM097 potently and selectively inhibited the proliferation of human AML cell lines and the majority of primary AML cells expressing wt p53, but not mutant p53, in a target-specific manner. Several patient samples that harbored mutant p53 were comparatively unresponsive to CGM097. Synergy was observed when CGM097 was combined with FLT3 inhibition against oncogenic FLT3-expressing cells cultured both in the absence as well as the presence of cytoprotective stromal-secreted cytokines, as well as when combined with MEK inhibition in cells with activated

⁶Corresponding authors: Ellen Weisberg, Ph.D., Department of Medical Oncology, Dana-Farber Cancer Institute, 450 Brookline Avenue, Boston, MA 02215, Mailstop: Mayer 540, Phone: (617)-632-3575, Fax: (617)-632-4388, ellen_weisberg@dfci.harvard.edu, Prof. James D. Griffin, M.D., Department of Medical Oncology, Dana-Farber Cancer Institute, 44 Binney Street, Boston, MA 02215, Mailstop: Mayer 540, Phone: (617)-632-3360, Fax: (617)-632-4388, james_griffin@dfci.harvard.edu.

*These authors contributed equally to this manuscript

** Current address: Atsushi Nonami, Center for Cellular and Molecular Medicine, Kyushu University Hospital 3-1-1 Maidashi, Higashi-ku, Fukuoka, Japan, 812-8582

*** Current address: Tao Ren, Decans Medical Devices Co. Ltd. Jiaxing City, Zhejiang, China 314031

**** Current address: Takaomi Sanda, Department of Medicine, National University of Singapore, Singapore 117599

***** Current address: Erik Nelson, Research Programs, The Leukemia & Lymphoma Society, White Plains, NY 10605

***** Current address: Sean McDonough, EMD Serono, Inc., Technology PI, Rockland, MA 02370

Conflict of Interest: J.D. Griffin receives research support and has a financial interest with Novartis Pharma AG. None of the authors included in this manuscript have a financial conflict of interest.

MAPK signaling. Finally, CGM097 was effective in reducing leukemia burden *in vivo*. These data suggest that CGM097 is a promising treatment for AML characterized as harboring wt p53 as a single agent, as well as in combination with other therapies targeting oncogene-activated pathways that drive AML.

Keywords

acute myeloid leukemia; p53; HDM2; tyrosine kinase inhibitor; apoptosis; synergy

Introduction

The p53 proto-oncogene is a transcription factor that controls the expression of a multitude of target genes involved in DNA repair, apoptosis and cell cycle arrest, which are all important phenomena counteracting the malignant growth of tumors. Dubbed “guardian of the genome,” p53 is thus critical for maintaining genetic stability, prohibiting defective cells from dividing and preventing tumor development (1).

While higher p53 expression correlates with induction of apoptosis and lower p53 expression correlates with inhibition of cell cycle progression (2–3), it is the cooperative binding of p53 to apoptosis-inducing genes versus cell cycle arrest genes that substantially contributes to cellular fate (4). p53-induced apoptosis is mediated by pro-apoptotic factors including phorbol-12-myristate-13-acetate-induced protein 1 (PMAIP1; NOXA), and p53-upregulated modulator of apoptosis (PUMA), which bind to anti-apoptotic proteins including Bcl-2 family members (5–6).

Mutations in p53 that disrupt its activity are found in more than 50% of all human malignancies, which makes p53 the most frequently mutated gene in transformed cells in humans. In cancers in which the p53 gene is not mutated, the function of the p53 pathway is often suppressed through mechanisms that affect its stability and activity. One such mechanism is overexpression or deregulation of MDM2. MDM2, for which the human orthologue is known as HDM2, is an E3 ubiquitin ligase which - by direct binding⁸- negatively regulates p53 through its ubiquitination and subsequent proteasome degradation (7–8).

Different strategies to restore p53 function in tumors, including acute leukemia, have been attempted. These include the design of antagonists (small molecule and peptides) to prevent interaction of wt p53 with its negative regulators, such as HDM2 (9–13), design of molecules that directly reactivate mutant p53 (14), and exogenous wt p53 expression, e.g., via adenovirus-mediated gene transfer (reviewed in 15). Two studies in transgenic mice, in which p53 expression was reversibly switched on and off, have independently shown that restoration of p53 function can lead to tumor regression *in vivo*, indicating that reactivating p53 is a promising therapeutic strategy (16–17).

Inhibition of the p53-HDM2 protein-protein interaction using small molecules as a means to antagonize negative regulators of p53 and thus activate p53 has been focused on targeting the p53 binding pocket of HDM2. The first HDM2 inhibitor to be developed was 4,5-

dihydroimidazole, also known as Nutlin (9). Further structure based optimization of Nutlin compounds yielded RG7112 and RG7388 (Roche). These compounds have recently been shown to lead to pharmacological p53 pathway activation and downstream signaling in human tumor tissue (18–19) and demonstrated initial signs of efficacy in patients with solid and hematologic malignancies (20). Several other chemical classes of HDM2 inhibitors have been developed, among which those that advanced into Phase I clinical development include AMG232 (Amgen), MI-773 (Sanofi), DS-30326 (Daiichi Sankyo), and MK842 (Merck) (13,21).

Early clinical trials with advanced-stage HDM2 inhibitors was limited by toxicity of these compounds (reviewed in 13). Even though HDM2 has been validated as a promising target for drug development, previous results warrants the identification and development of novel, more potent and efficacious HDM2 inhibitors with less toxic side effects. Here, we introduce the Novartis HDM2 inhibitor, CGM097, as a potent inhibitor of wt p53-expressing AML that has the potential to be used alone or in combination with conventional therapies, such as Ara-C (cytarabine), or other oncogene-targeted therapies for AML.

Materials and Methods

Cell lines and cell culture

OCI-AML3, OCI-AML5, P31-FUJ, SKM-1, NOMO-1, and NB4 were obtained from Dr. Gary Gilliland. HEL, HL60, KG-1, Kasumi-1, KU812F, U937, MONOMAC6, and SKNO-1 were purchased from the American Type Culture Collection (ATCC) (Manassas, VA, USA). MOLM-13 (DSMZ (German Resource Centre for Biological Material), was engineered to express luciferase fused to neomycin phosphotransferase (pMMP-LucNeo) by transduction with a VSVG-pseudotyped retrovirus as previously described (22). MOLM-14 (23) was provided by Dr. Scott Armstrong, Dana Farber Cancer Institute, Boston, MA.

OCI-AML3 cells were cultured in alpha MEM media (Mediatech, Inc, Herndon, VA) +10% fetal bovine serum (FBS) + 2% L-glutamine + 1% penicillin/streptomycin. OCI-AML5 cells were cultured in RPMI + 10% FBS + 2% L-glutamine + 1% penicillin/streptomycin, and supplemented with GM-CSF. All other lines were cultured in RPMI (Mediatech, Inc., Herndon, VA) +10% FBS + 2% L-glutamine + 1% penicillin/streptomycin. Cells were cultured in 5% CO₂ at 37°C at a concentration of 2×10⁵ to 5×10⁵.

We have authenticated the following cell lines through cell line short tandem repeat (STR) profiling (DDC Medical, Fairfield, OH): MOLM14, NOMO-1, HEL, SKM-1, OCI-AML3, and NB4. All cell lines matched >80% with lines listed in the DSMZ Cell Line Bank STR Profile Information. Other cell lines expressing mutated RAS or wild-type RAS were sequenced or tested with pharmacological inhibitors for validation of cell line integrity (24). All cell lines were obtained between 2000 and 2015.

Chemical compounds and biologic reagents

CGM097 and PKC412 were synthesized by Novartis Pharma AG, Basel, Switzerland. AZD6244 and AC220 were purchased from MedChem Express Co. Ltd. Compounds were

initially dissolved in DMSO to make 10 mM stock solutions, and then were serially diluted to obtain final concentrations for *in vitro* experiments.

AML patient cells

Frozen vials of bone marrow from AML patients identified as harboring mutant FLT3 were thawed prior to processing. Mononuclear cells were isolated from normal bone marrow by density gradient centrifugation through Ficoll-Plaque Plus (Amersham Pharmacia Biotech AB, Uppsala, Sweden) at 2000 rpm for 30 minutes, followed by two washes in 1× PBS. Mononuclear cells were then tested in liquid culture (Iscove's MDM, supplemented with 20% FCS). All bone marrow samples from AML patients were obtained under approval of the Dana-Farber Cancer Institute Institutional Review Board. Patient information is provided in Supplementary Table I.

Elisa assay

MIC-1 ELISAs were performed using the Quantikine ELISA assay Human GDF-15 (R&D systems) as follows: After culturing cells with DMSO or CGM097 for 2–3 days, supernatants were harvested and incubated in the assay plate for 2 hrs. Bound protein was probed with a primary antibody against MIC-1, and absorbance was measured on a spectrophotometer (Molecular Devices, Sunnyvale, California) following addition of secondary antibody conjugated to HRP.

Proliferation studies, apoptosis assays, and cell cycle analysis

Cell counts for proliferation studies were obtained using the trypan blue exclusion assay, as previously described (24). Error bars represent the standard error of the mean for each data point. Programmed cell death of inhibitor-treated cells was determined using the Annexin-V-Fluos Staining Kit (Boehringer Mannheim, Indianapolis, IN), as previously described (24). Cell cycle analysis was performed as previously described (24).

Drug combination studies

For drug combination studies, compounds were added simultaneously at fixed ratios to cells, and cell viability was determined by trypan blue exclusion and expressed as the function of growth affected (FA) drug-treated versus control cells. Synergy was assessed by Calcsyn software (Biosoft, Ferguson, MO and Cambridge, UK), using the Chou-Talalay method (25). The combination index = $[D]_1 / [D_x]_1 + [D]_2 / [D_x]_2$, where $[D]_1$ and $[D]_2$ are the concentrations required by each drug in combination to achieve the same effect as concentrations $[D_x]_1$ and $[D_x]_2$ of each drug alone.

Colony Assays

Soft agar colony assays utilized an upper layer of 3% Noble agar (Difco, Lawrence, KS) in IMDM (HyClone, Logan, UT), supplemented with FCS and L-glutamine, and a lower layer of 5% Noble agar in IMDM medium, also supplemented with FCS and L-glutamine, in each well of a 24-well plate. Agar was liquefied by microwaving, and then heated at 55°C prior to cooling to 45°C before plating and solidifying. Colonies were allowed to grow for >2 weeks prior to counting.

Genotyping

Ten exons were amplified by PCR with exon-specific primers. PCR reactions were set up in 25 μ L volume reaction containing 100 ng of genomic DNA, 0.4 μ mol/l of each primer and 1 U Taq DNA Platinum High Fidelity polymerase (Invitrogen cat#11304-029). After a denaturation step of 2 minutes at 94°C, the PCR consisted of 35 cycles of 30 seconds at 94°C, 30 seconds at 54°C, and 1 minute 30 seconds at 68°C. The resulting PCR products were evaluated on a 1% agarose gel. After purification of PCR products using an extraction kit (QiaQuick Gel Extraction Kit; Qiagen), sequencing analysis in both directions was performed by either (1) using a BigDye® Terminator v3.1 Cycle Sequencing Kit and 3730 DNA Analyzer (Applied Biosystems®) with 10 pmoles of sequencing primer (Boston University), or (2) inhouse Sanger sequencing with 10 pmoles of sequencing primer (Novartis Pharmaceuticals). Amplification and sequencing primers are shown in Supplementary Figure 1.

Yeast-based p53 functional assay

The yeast-based p53 functional assay utilizes human p53 expressed in *Saccharomyces cerevisiae*, which activates ADE2 gene transcription (26). The assay tests the critical biological function of p53 and can distinguish inactivating mutations from functionally silent mutations. Dr. Richard Iggo of the Bergonie Cancer Institute, University of Bordeaux, France, kindly provided us with the yeast strain, YIG397, and pRDI-22 plasmid required for this assay.

Briefly, p53 mRNA was isolated from cell lines or primary AML samples and reverse transcribed and amplified by PCR using the following primers:

P3: [5'-ATT-TGA-TGC-TGT-CCC-CGG-ACG-ATA-TTGAA(S)C-3',

P4: 5'-ACC-CTT-TTT-GGA-CTT-CAG-GTG-GCTGGA- GT(S)G]

To test p53 status, yeast IG397 were co-transformed with unpurified RT-PCR product, linearized vector (pRDI-22 cut by HindIII and StudI), and carrier DNA by the lithium acetate procedure (27), plated on synthetic minimal medium minus leucine plus adenine (5 μ g/mL), and incubated for 2-3 days at 35°C. Specifically, gap repair of the plasmid with the PCR product leads to constitutive expression of the human p53 protein. Yeast expressing repaired plasmids are selected on medium that lacks leucine but that contains just enough adenine for Ade- cells to grow. These yeast colonies, which contain mutant p53, are red. In contrast, colonies containing wt p53 are white. Red colonies are clearly identifiable after 2–3 days at 35°C, however the color is more intense after an additional two days at 4°C.

In vivo study

Model development and efficacy study—The AML patient-derived mouse model was developed by intravenously (IV) implanting patient peripheral blood mononuclear cells (PBMCs) into 8 week-old female NSG mice (The Jackson Laboratory, Bar Harbor, Maine) (5 million cells/mouse in 0.2 ml PBS). The model was serially transplanted twice in mice before initiation of the efficacy study. For the efficacy study, 21 NSG mice were implanted

IV with 5 million cells in PBS each in a total volume of 0.2 ml/mouse. Leukemic tumor burden was measured twice weekly by FACS analysis of % human CD45⁺ cells in mouse blood as described below. Body weights were measured twice weekly and clinical observations were recorded. At 35 days post-implant, mice were randomized into 3 different groups with a mean leukemic burden of approximately 18% CD45⁺ cells per group (n=7/group). CGM097 (100 mg/kg po qd) was administered in a volume of 10 ml/kg. ARA-C (Cytarabine) was purchased from Selleckchem (Houston, TX, Catalog number S1648) and administered intraperitoneally (IP) in a volume of 10 ml/kg at the dose of 50 mg/kg qd.

NSG female mice were purchased from The Jackson Laboratory (Bar Harbor, Maine) and were allowed to acclimate in the Novartis NIBRI animal facility with access to food and water ad libitum for a minimum of 3 days prior to manipulation. Handling of mice and procedures described in this manuscript were in accordance with Novartis ACUC regulations and guidelines.

FACS analysis

Mouse blood (via tail vein nick) was collected into EDTA coated capillary tubes (purple tops, Sarstedt P/N: 16.444.100) and 20 µl was aliquoted into a 96 well plate (BD P/N: 351177) containing 200 µl 1× RBC Lysis Buffer at room temperature for 5 minutes. The plate underwent centrifugation at 1200 RPM for 5 minutes and supernatant was discarded. This step was repeated twice after which cells were re-suspended in 2% FBS in PBS, centrifuged at 1200 RPM for 5 minutes and blocked with mouse and human Fc Blocking Reagents (1:20 dilution) (Miltenyi P/N's 130-092-575 and 130-059-091) for 10–30 minutes on ice. Samples were next incubated with either CD45-APC (eBioscience P/N: 17-9459-42) or APC isotype control (eBioscience P/N: 17-4714-42) antibody diluted in 2% FBS in PBS (1:200) for 30–60 minutes on ice in a dark room. Following antibody incubation, samples were washed twice in 2% FBS in PBS, re-suspended in a final volume of 100 µl 2% FBS in PBS and processed for FACS analysis (BD FACSCanto II with 3 lasers - 488–561–635 nm). Data were analyzed via FlowJo and reported as % hCD45⁺ cells within mouse PBMCs.

Tumor Volume Data Analysis

Tumor burden was determined by % hCD45⁺ cells present in mouse blood using FACS analysis methods described above.

Percent treatment/control (T/C) values were calculated using the following formula:

$$\%T/C = 100 \times T / C$$

where:

T = mean tumor volume of the drug-treated group on the final day of the study;

T = mean tumor volume of the drug-treated group on the final day of the study – mean tumor volume of the drug-treated group on initial day of dosing;

C = mean tumor volume of the control group on the final day of the study; and

C = mean tumor volume of the control group on the final day of the study – mean tumor volume of the control group on initial day of dosing.

All data were expressed as mean and SEM. Significance was determined using two tailed unpaired student's t test. Statistical analysis was carried out using GraphPad Prism (GraphPad Software Inc., La Jolla, CA).

Results

CGM097 inhibits proliferation of wt p53-expressing AML via induction of apoptosis and inhibition of cell cycle progression

We investigated the activity of the small molecule HDM2 inhibitor, CGM097 (the chemical structure is depicted in Figure 1A), against a panel of wt p53-expressing human AML cell lines (MOLM13, MOLM14, OCI-AML3, OCI-AML5) and mutant p53-expressing human AML cell lines (HL60, HEL, KG1, U937, NB4, MONOMAC6, Kasumi-1, SKNO-1 and P31) (Figure 1B and Supplementary Table II). We found a positive correlation between wt p53 and good response to CGM097, whereas the opposite was true for mutant p53-expressing cells. CGM097 inhibition of proliferation of wt p53-expressing cell lines correlated with CGM097 induction of apoptosis (Figure 1C and Supplementary Figure 2) and G1 arrest (Figure 1D and Supplementary Figure 3), suggesting that programmed cell death and inhibition of cell cycle progression contribute to the growth inhibitory effects of CGM097.

In order to investigate the potential of CGM097 to be used clinically, we tested the drug against 19 AML samples, the majority of which were characterized as expressing wt p53. We observed CGM097 to display substantial activity against the wt p53-expressing samples, with little-to-no activity against mutant p53-expressing samples (Figure 2A and Supplementary Table III). The difference in response to CGM097 between wt p53-expressing samples and mutant p53-expressing samples was statistically significant ($p=0.01$). In addition, 10 of 16 wt p53-expressing AML patient samples showed significantly higher responsiveness to CGM097 (near or over 50% drug-induced killing at 500 nM) when compared to normal bone marrow samples, 4/4 of which showed less than 50% killing (Figure 2A–B) ($p=0.0004$). These data suggest that CGM097 is efficacious toward wt p53-expressing AML.

We adapted and utilized a simple yeast-based p53 functional assay²⁶ to validate the wt versus mutant p53 status in two wt p53-expressing AML patient samples that were tested for responsiveness to CGM097, as well as control cell lines expressing wt or mutant p53. As shown in Figure 2C, this assay did, indeed, confirm the expression of wt p53 in these patient samples, a finding which also substantiates the utility of this assay as a complementary approach to genotyping.

CGM097 displayed a range of potencies against the wt p53-expressing AML patient samples. For example, all of the patient samples characterized as expressing wt p53 responded to 1000 nM CGM097 with significantly higher cell killing than mutant p53-expressing samples or KU812F cells (KU812F was used as a negative control for comparison due to expression of mutant p53 in this line). Among the wt p53-expressing patient samples, a large fraction were very sensitive, with IC₅₀ values below 250 nM, while others showed IC₅₀s of up to 1000 nM. This would indicate that even though CGM097 is

highly active in some wt p53 patients, the efficacy of this drug can be potentially influenced by other oncogenic drivers, signaling pathways or drug resistance mechanisms.

CGM097 selectively augments p53 activity in wt p53-expressing AML

The transforming growth factor- β superfamily cytokine, macrophage inhibitory cytokine-1 (MIC-1), serves as a secreted biomarker for p53 activation in cancer (28). An ELISA assay was employed to measure secreted MIC-1 in media collected from normal bone marrow cells or the wt p53-expressing AML cell line, MOLM14, treated with 0, 250, and 500 nM CGM097. We observed CGM097 to selectively increase MIC secretion by MOLM14 cells but not normal human bone marrow, despite the expression of wt p53 in the normal bone marrow samples (Figure 3A). Similarly, CGM097 selectively increased MIC-1 secretion by wt p53-expressing OCI-AML3 cells but not mutant p53-expressing HEL cells (Figure 3B). These results further validate the target specificity of CGM097 towards wt, but not mutant, p53 in leukemic cells.

CGM097 synergizes with TKIs against oncogene-driven AML

We were also interested in testing the ability of CGM097 to synergize with a FLT3 inhibitor, presuming dual suppression of oncogenic FLT3 and induction of tumor suppressive wt p53. To address this, we first used FLT3-ITD-expressing MOLM13 cells, the proliferation and soft agar colony growth of which are potently inhibited by CGM097 (Supplementary Figure 4). The combination of the broad spectrum FLT3 inhibitor, PKC412, and CGM097 led to more killing of MOLM13 cells than either drug alone and was found to be nearly additive (ED50) to synergistic (ED75-ED90) (Supplementary Figure 5). We also tested the drug combination against MOLM14 cells and observed synergy (Figure 4A). Similarly, the combination of CGM097 and a more highly selective inhibitor of FLT3, AC220, led to synergy against mutant FLT3-positive cells (Table I and Supplementary Figure 6). Synergy between FLT3 inhibition and CGM097 correlated with up-regulation of expression levels of pro-apoptotic p53 upregulated modulator of apoptosis (PUMA) (Figure 4E) and down-regulation of anti-apoptotic Myeloid cell leukemia-1 (Mcl-1) (Figure 4F).

Since co-culturing AML cells with stroma leads to upregulation of anti-apoptotic proteins (29), use of a p53 activator (pro-apoptotic) should help to counteract this. This led us to explore the combination of CGM097 with either PKC412 or AC220 against mutant FLT3-positive cells cultured in the presence of 90% stromal-conditioned media (SCM) from the human stromal cell lines, HS-5 or HS27a. We observed HS-5-derived SCM or HS27a-derived SCM to confer partial protection to PKC412 or AC220-treated mutant FLT3-positive cells (Figure 4D and Supplementary Figure 6). Addition of CGM097 was able to counteract the SCM-induced protection from FLT3 inhibitors. In fact, the combination of CGM097 and PKC412 or CGM097 and AC220 was synergistic against mutant FLT3-positive cells cultured in the presence of SCM. This synergy was comparable to that observed for these drug combinations against mutant FLT3-positive cells cultured in the presence of RPMI+10% FBS (Figure 4B–C, Table I and Supplementary Figure 6).

Analysis of AML patient samples suggests that mutant RAS and mutant p53 are in general mutually exclusive (30). Consequently, we were interested in testing the ability of CGM097

to synergize with a downstream inhibitor of RAS signaling, presuming a combined effect of suppressing mutant RAS and inducing wt p53. NRAS mutant, p53 wt human primary AML sample (AML #10) showed a modest response to CGM097 alone. The modest response of the mutant RAS-expressing patient sample further prompted us to investigate the ability of RAS pathway inhibition and wt p53 activation to synergize. Similar to previous work that showed synergy between the MEK inhibitor AZD6244 (Selumetinib) and nutlin (31), we also observed AZD6244 and CGM097 to synergistically inhibit proliferation and induce apoptosis in mutant NRAS-expressing OCI-AML3 cells (Figure 5A–C and Supplementary Figure 7).

CGM097 shows activity in vivo against wt p53-expressing AML

To determine the activity of HDM2 inhibition *in vivo*, CGM097 was tested in a p53 wt AML patient-derived mouse xenograft (Figure 6). Treatment of tumor bearing mice began when mice exhibited 18% tumor burden (measured by FACS analysis of hCD45). Tumor burden decreased upon initiation of CGM097 treatment and remained regressed until the end of study. On Day 69, the last day of an intact vehicle control group, CGM097 resulted in tumor regression with % T/ C of –26%, $p < 0.05$ (Figure 6A). Treatment of mice with standard of care (SOC) agent ARA-C also resulted in tumor regression with % T/ C of –25.5%, $p < 0.05$. However, after 15 consecutive doses with ARA-C, mice exhibited significant body weight loss and treatment was discontinued. In contrast, treatment with CGM097 was well tolerated, and body weight loss was not observed (Figure 6B). Return of disease was not measured upon discontinuing CGM097 treatment. It should also be noted that CGM097 displays species specificity toward human and not murine MDM2 (32). Nonetheless, these data show striking anti-tumor efficacy of CGM097 in the AML patient derived xenograft model. Taken together with data shown for cell lines as well as patient samples, the results suggest that CGM097 is an effective agent in inhibiting p53 wt-expressing AML

Discussion

p53 protein levels are strictly regulated and are suppressed by a negative regulator of p53, the E3 ubiquitin protein ligase MDM2 (7). MDM2 interacts with p53 through direct binding to the p53 amino terminus; the binding of MDM2 to p53 makes p53 a target for ubiquitylation and consequent protein degradation (7). Small molecule inhibitors and peptides have been developed to inhibit the association between HDM2 and p53 by targeting the p53 pocket of HDM2, thereby blocking the interaction between p53 and HDM2 and consequently stabilizing p53 such that its tumor suppressor activity is renewed (9, 33–37).

Since p53 mutations in AML are rare and AML is in need of new and improved treatment strategies, this is an ideal disease target for small molecule inhibitors of MDM2. Indeed, preclinical studies with nutlin-3 have shown activity in AML (10–12). Here, we introduce the novel HDM2 inhibitor, CGM097, which displayed substantial activity against wt p53-expressing AML cell lines and selective toxicity toward primary AML cells expressing wt p53.

The synthesis and binding affinity to MDM2 of CGM097 have been described and disclosed (38). Briefly, a screen of 50,000 compounds exploiting a three hotspot 2D/3D

pharmacophore led to identification of a series of isoquinolinones, the subsequent optimization of which revealed a novel binding mode with changes in protein organization associated with His 96 interactions (38). Additional changes resulted in the clinical candidate CGM097, a substituted 1,2-dihydroisoquinolinone derivative designed to mimic three key hydrophobic interactions made by p53 residues with Phe19, Trp23 and Leu26 in the HDM2 pocket (8, 39). CGM097 (structure revealed in 38, 40) binds to the p53 pocket of HDM2 with high potency and exceptional selectivity; in biochemical assays, CGM097 displaces the p53 peptide from the surface of HDM2 with an IC_{50} of 1.7 nM, compared with an IC_{50} of 2,000 nM for HDMX (38, 40). In a cell proliferation assay, CGM097 inhibited the growth of HCT-116 p53^{WT} cells with a GI_{50} of 454 nM and of HCT-116 p53-null cells with a GI_{50} of 15,983 nM (38, 40). In contrast to HDM2 inhibitors, such as nutlin-3, which have been shown to display limited bioavailability in oral formulations in preclinical models (41), CGM097 is well-absorbed with a moderate to high oral bioavailability ranging from 57 to 81% across multiple animal species tested (mouse, rat, dog and monkey) (38, 42). In addition, CGM097 displays an excellent PK profile, low human intrinsic clearance, and exceptional ability to selectively inhibit p53/Mdm2 over p53/Mdm4 with negligible activity against p53 null cells^{38,40,42}. Lastly, CGM097 demonstrates dose-dependent anti-tumor activity in human primary tumor xenografts in a p53 dependent manner (38, 40, 42).

Therapies aimed at restoring activation of p53 to replenish its tumor suppressive role in malignancies carry the risk of p53-induced apoptosis in normal cells. However, it has been shown that a level of p53 activation can potentially be achieved through tight regulation of its duration and strength that is not toxic to normal tissues but that still allows tumor suppression (43–48). In support of this, minimal toxicity in preclinical mouse models was observed with Roche HDM2 inhibitors due to their short cellular presence and transient p53 stimulation; however a lower binding affinity of these drugs, which were optimized for human MDM2, toward mouse MDM2 could not be ruled out as being responsible for this lower toxicity (19, 38). Indeed, adverse reactions and modest efficacy were associated with clinical testing of the Roche HDM2 inhibitor, RG7112 (18). In addition, mutations conferring resistance to MDM2 inhibitors have been identified in preclinical studies (49–50). This suggests a need for identification and development of novel MDM2 inhibitors, as well as perhaps new MDM2 inhibitor-associated combination therapy approaches that may be more efficacious than MDM2 inhibition alone.

CGM097 exhibits 8-fold greater affinity for MDM2 over Nutlin-3 (32). Importantly, as shown in this report, CGM097 displayed little toxicity toward normal bone marrow samples while potently and selectively inhibiting the proliferation and viability of wt p53-expressing primary AML patient cells and AML cell lines. In vivo testing using a primagraft model suggested high sensitivity of primary AML patient cells to CGM097 inhibition, as after only a week of consecutive dosing, there were 0% of hCD45+ cells in all mice (n=7) compared to 18% at the start of treatment. At the end of the experiment (69 days post tumor implantation), untreated mice had 87% hCD45+cells present in their blood, while the % hCD45+cells in mice treated with CGM097 remained at 0%.

These encouraging preclinical results support the clinical testing of CGM097 in AML patients. Presently, CGM097 is being investigated in a Phase I dose escalation study in adult patients with selected advanced solid tumors expressing wt p53.

We also show the ability of CGM097 to synergize with selectively inhibitory TKIs, including inhibitors of mutant FLT3 and RAS-mediated signaling, even in the presence of secreted cytoprotective stroma-derived cytokines. These results suggest that CGM097 could potentially be used in combination with other targeted agents against oncogene-driven AML, as well as synergize in the presence of growth promoting factors and potentially override stromal-mediated drug resistance. Taken together, our findings support the further development of CGM097 as a potential novel therapeutic, alone or in combination with other targeted therapies for the treatment of AML.

Supplementary Material

Refer to Web version on PubMed Central for supplementary material.

Acknowledgement

We would like to thank Amanda L. Christie for her assistance with statistical analysis.

Grant Support: J.D. Griffin received NIH grant CA66996 and the work of all authors (with the exception of employees of Novartis Pharmaceuticals and M. Sattler) related to CGM097 was supported by this grant. M. Sattler received NIH grant CA134660-03. E. Halilovic, V.G. Cooke, J. Yuan, B. Antonakos, L. Barys, M. Ito, S. Jeay, J.U. Wuerthner, and M. Wiesmann are employees of Novartis Pharmaceuticals.

References

1. Lane DP. p53, guardian of the genome. *Nature*. 1992; 358:15–16. [PubMed: 1614522]
2. Chen X, Ko LJ, Jayaraman L, Prives C. p53 levels, functional domains, and DNA damage determine the extent of the apoptotic response of tumor cells. *Genes Dev*. 1996; 10:2438–2451. [PubMed: 8843196]
3. Kracikova M, Akiri G, George A, Sachidanandam R, Aaronson SA. A threshold mechanism mediates p53 cell fate decision between growth arrest and apoptosis. *Cell Death Differ*. 2013; 20:576–588. [PubMed: 23306555]
4. Schlereth K, Charles JP, Bretz AC, Stiewe T. Life or death: p53-induced apoptosis requires DNA binding cooperativity. *Cell Cycle*. 2010; 9:4068–4076.
5. Villunger A, Michalak EM, Coultas L, Mullauer F, Bock G, Ausserlechner MJ, et al. p53- and drug-induced apoptotic responses mediated by BH3-only proteins puma and noxa. *Science*. 2003; 302:1036–1038. [PubMed: 14500851]
6. Chen L, Willis SN, Wei A, Smith BJ, Fletcher JI, Hinds MG, et al. Differential targeting of prosurvival Bcl-2 proteins by their BH3-only ligands allows complementary apoptotic function. *Mol. Cell*. 2005; 17:393–403. [PubMed: 15694340]
7. Honda R, Tanaka H, Yasuda H. Oncoprotein MDM2 is a ubiquitin ligase E3 for tumor suppressor p53. *FEBS Lett*. 1997; 420:25–27. [PubMed: 9450543]
8. Kussie PH, Gorina S, Marechal V, Elenbaas B, Moreau J, Levine AJ, et al. Structure of the MDM2 oncoprotein bound to the p53 tumor suppressor transactivation domain. *Science*. 1996; 274:948–953. [PubMed: 8875929]
9. Vassilev LT, Vu BT, Graves B, Carvajal D, Podlaski F, Filipovic Z, et al. In vivo activation of the p53 pathway by small-molecule antagonists of MDM2. *Science*. 2004; 303:844–848. [PubMed: 14704432]

10. Secchiero P, Zerbinati C, di lasio MG, Melloni E, Tiribelli M, Grill V, et al. Synergistic cytotoxic activity of recombinant TRAIL plus the non-genotoxic activator of the p53 pathway nutlin-3 in acute myeloid leukemia cells. *Current Drug Metabolism*. 2007; 8:395–403. [PubMed: 17504227]
11. Secchiero P, Melloni E, di lasio MG, Tiribelli M, Rimondi E, Corallini F, et al. Nutlin-3 up-regulates the expression of Notch1 in both myeloid and lymphoid leukemic cells, as part of a negative feedback antiapoptotic mechanism. *Blood*. 2009; 113:4300–4308. [PubMed: 19190243]
12. Secchiero P, Bosco R, Celeghini C, Zauli G. Recent advances in the therapeutic perspectives in nutlin-3. *Current Pharmaceutical Design*. 2011; 17:569–577. [PubMed: 21391907]
13. Khoo KH, Verma CS, Lane DP. Drugging the p53 pathway: understanding the route to clinical efficacy. *Nat Rev Drug Discov*. 2014; 13:217–236. [PubMed: 24577402]
14. Liu X, Wilcken R, Joerger AC, Chuckowree IS, Amin J, Spencer J, et al. Small molecule induced reactivation of mutant p53 in cancer cells. *Nucleic Acids Res*. 2013; 41:6034–6044. [PubMed: 23630318]
15. Roth JA. Adenovirus p53 gene therapy. *Expert Opin Biol Ther*. 2006; 6:55–61. [PubMed: 16370914]
16. Martins CP, Brown-Swigart L, Evan GI. Modeling the therapeutic efficacy of p53 restoration in tumors. *Cell*. 2006; 127:1323–1334. [PubMed: 17182091]
17. Ventura A, Kirsch DG, McLaughlin ME, Tuveson DA, Grimm J, Lintault L, et al. Restoration of p53 function leads to tumor regression in vivo. *Nature*. 2007; 445:661–665. [PubMed: 17251932]
18. Ray-Coquard I, Blay JY, Italiano A, Le Cesne A, Penel N, Zhi J, et al. Effect of the MDM2 antagonist RG7112 on the p53 pathway in patients with MDM2-amplified, well-differentiated or dedifferentiated liposarcoma: an exploratory proof-of-mechanism study. *Lancet Oncol*. 2012; 13:1133–1140. [PubMed: 23084521]
19. Ding Q, Zhang Z, Liu JJ, Jiang N, Zhang J, Ross TM, et al. Discovery of RG7388, a potent and selective p53-MDM2 inhibitor in clinical development. *J Med Chem*. 2013; 56:5979–5983. [PubMed: 23808545]
20. Andreeff M, Kelly KR, Yee K, Assouline S, Strair R, Popplewell L, et al. Results of the Phase I trial of RG7112, a small-molecule MDM2 antagonist, in acute leukemia. *Blood*. 2012 (suppl; abst 675).
21. Sun D, Li Z, Rew Y, Gribble M, Bartberger MD, Beck HP, et al. Discovery of AMG 232, a potent, selective, and orally bioavailable MDM2-p53 inhibitor in clinical development. *J Med Chem*. 2014; 57:1454–1472. [PubMed: 24456472]
22. Armstrong SA, Kung AL, Mabon ME, Silverman LB, Stam RW, Den Boer ML, et al. Validation of a therapeutic target identified by gene expression based classification. *Cancer Cell*. 2003; 3:173–183. [PubMed: 12620411]
23. Matsuo Y, MacLeod RA, Uphoff CC, Drexler HG, Nishizaki C, Katayama Y, et al. Two acute monocytic leukemia (AML-M5a) cell lines (MOLM13 and MOLM14) with interclonal phenotypic heterogeneity showing MLL-AF9 fusion resulting from an occult chromosome insertion, ins(11;9)(q23;p22p23). *Leukemia*. 1997; 11:1469–1477. [PubMed: 9305600]
24. Nonami A, Sattler M, Weisberg E, Liu Q, Zhang J, Patricelli MP, et al. Identification of novel therapeutic targets in acute leukemias with NRAS mutations using a pharmacologic approach. *Blood*. 2015; 125:3133–3143. [PubMed: 25833960]
25. Chou TC and Talalay P. Quantitative analysis of dose-effect relationships: the combined effects of multiple drugs or enzyme inhibitors. *Adv Enzyme Regul*. 1984; 22:27–55. [PubMed: 6382953]
26. Flaman JM, Frebourg T, Moreau V, Charbonnier F, Martin C, Chappuis P, et al. A simple p53 functional assay for screening cell lines, blood, and tumors. *Proc Natl Acad Sci USA*. 1995; 92:3963–3967. [PubMed: 7732013]
27. Ishioka C, Frebourg T, Yan YX, Vidal M, Friend SH, Schmidt S, et al. Screening patients for heterozygous p53 mutations using a functional assay in yeast. *Nat. Genet*. 1993; 5:124–129. [PubMed: 8252037]
28. Yang H, Filipovic Z, Brown D, Breit SN, Vassilev LT. Macrophage inhibitory cytokine-1: a novel biomarker for p53 pathway activation. *Mol Cancer Ther*. 2003; 2:1023–1029. [PubMed: 14578467]

29. Konopleva M, Konoplev S, Hu W, Zaritskey AY, Afanasiev BV, Andreeff M. Stromal cells prevent apoptosis of AML cells by up-regulation of anti-apoptotic proteins. *Leukemia*. 2002; 16:1723–1724.
30. Cancer Genome Atlas Research Network. Genomic and epigenomic landscapes of adult de novo acute myeloid leukemia. *N Engl J Med*. 2013; 368:2059–2074. [PubMed: 23634996]
31. Zhang W, Konopleva M, Burks JK, Dywer KC, Schober WD, Yang JY, et al. Blockade of mitogen-activated protein kinase/extracellular signal-regulated kinase and murine double minute synergistically induces apoptosis in acute myeloid leukemia via BH3-only proteins Puma and Bim. *Cancer Res*. 2010; 70:2424–2434. [PubMed: 20215498]
32. Valat T, Masuya K, Baysang F, Albrecht G, Buschmann N, Erdmann D, Furet P, et al. Mechanistic study of NVP-CGM097: a potent, selective and species specific inhibitor of p53-Mdm2. *Cancer Res*. 2014; 75 (suppl; abstr 1798).
33. Bernal F, Tyler AF, Korsmeyer SJ, Walensky LD, Verdine GL. Reactivation of the p53 tumor suppressor pathway by a stapled p53 peptide. *J. Am. Chem. Soc.* 2007; 129:2456–2457. [PubMed: 17284038]
34. Koblisch HK, Zhao S, Franks CF, Donatelli RR, Tominovich RM, LaFrance LV, et al. Benzodiazepinedione inhibitors of the Hdm2:p53 complex suppress human tumor cell proliferation in vitro and sensitize tumors to doxorubicin in vivo. *Mol. Cancer Ther*. 2006; 5:160–169. [PubMed: 16432175]
35. Shangary S, Qin D, McEachern D, Liu M, Miller RS, Qiu S, et al. Temporal activation of p53 by a specific MDM2 inhibitor is selectively toxic to tumors and leads to complete tumor growth inhibition. *Proc. Natl. Acad. Sci. USA*. 2008; 105:3933–3938. [PubMed: 18316739]
36. Yin H, Lee G-i, Park HS, Payne GA, Rodriguez JM, Sebti SM, et al. Terpheyl-based helical mimetics that disrupt the p53/HDM2 interaction. *Angew. Chem. Int. Ed. Engl.* 2005; 44:2704–2707. [PubMed: 15765497]
37. Kritzer JA, Lear JD, Hodsdon ME, Schepartz A. Helical β -peptide inhibitors of the p53-hDM2 interaction. *J. Am. Chem. Soc.* 2004; 126:9468–9469. [PubMed: 15291512]
38. Collingwood SP, Ratcliffe AJ, Pryde D, Porter R. Recent disclosures of clinical candidates: Highlights from the Society of Medicines Research Symposium, held December 4, 2014- National Heart & Lung Institute, London, UK. *Drugs of the Future*. 2015; 40(1):81–91.
39. Furet P, Chene P, De Pover A, Valat TS, Lisztwan JH, Kallen J, et al. The central valine concept provides an entry in a new class of non peptide inhibitors of the p53-MDM2 interaction. *Bioorg Med Chem Lett*. 2012; 22:3498–3502. [PubMed: 22507962]
40. Jeay S, Gaulis S, Ferretti S, Bitter H, Ito M, Valat T, et al. A distinct p53 target gene set predicts for response to the selective p53-HDM2 inhibitor NVP-CGM097. *Elife*. 2015 May 12.4:e06498.
41. Zhang F, Tagen M, Throm S, Mallari J, Miller L, Guy RK, et al. Whole-body physiologically based pharmacokinetic model for nutlin-3a in mice after intravenous and oral administration. *Drug Metab Dispos*. 2011; 39:15–21. [PubMed: 20947617]
42. Ferretti, S.; Berger, M.; Rebmann, R.; Santacroce, F.; Sterker, D.; Jensen, M., et al. San Diego CA. Philadelphia (PA): AACR; 2014 Apr 5–9. NVP-CGM097: a novel p53-Mdm2 inhibitor exhibiting potent antitumor activity in mouse models of human cancer. *Cancer Res* 74, 2014 (19 suppl; abstr 4638).
43. Garcia-Cao I, Garcia-Cao M, Martin-Caballero J, Criado LM, Klatt P, Flores JM, et al. "Super p53" mice exhibit enhanced DNA damage response, are tumor resistant and age normally. *EMBO J*. 2002; 21:6225–6235. [PubMed: 12426394]
44. Mendrysa SM, McElwee MK, Michalowski J, O'Leary KA, Young KM, Perry ME. Mdm2 is critical for inhibition of p53 during lymphopoiesis and the response to ionizing irradiation. *Mol Cell Biol*. 2003; 23:462–472. [PubMed: 12509446]
45. Bond GL, Hu W, Bond EE, Robins H, Lutzker SG, Arva NC, et al. A single nucleotide polymorphism in the MDM2 promoter attenuates the p53 tumor suppressor pathway and accelerates tumor formation in humans. *Cell*. 2004; 119:591–602. [PubMed: 15550242]
46. Christophorou MA, Ringshausen I, Finch AJ, Swigart LB, Evan GI. The pathological response to DNA damage does not contribute to p53-mediated tumor suppression. *Nature*. 2006; 443:214–217. [PubMed: 16957739]

47. Mendrysa SM, Perry ME. Tumor suppression by p53 without accelerated aging: just enough of a good thing? *Cell Cycle*. 2006; 5:714–717. [PubMed: 16582632]
48. Van Leeuwen IM, Higgins M, Campbell J, Brown CJ, McCarthy AR, Pirrie L, et al. Mechanism-specific signatures for small-molecule p53 activators. *Cell Cycle*. 2011; 10:1590–1598. [PubMed: 21490429]
49. Michaelis M, Rothweiler F, Barth S, Cinatl J, van Rikxoort M, Loschmann N, et al. Adaptation of cancer cells from different entities to the MDM2 inhibitor nutlin-3 results in the emergence of p53-mutated multi-drug resistant cancer cells. *Cell Death Dis*. 2011; 2:e243. [PubMed: 22170099]
50. Aziz MH, Shen H, Maki CG. Acquisition of p53 mutations in response to the non-genotoxic p53 activator nutlin-3. *Oncogene*. 2011; 30:4678–4686. [PubMed: 21643018]

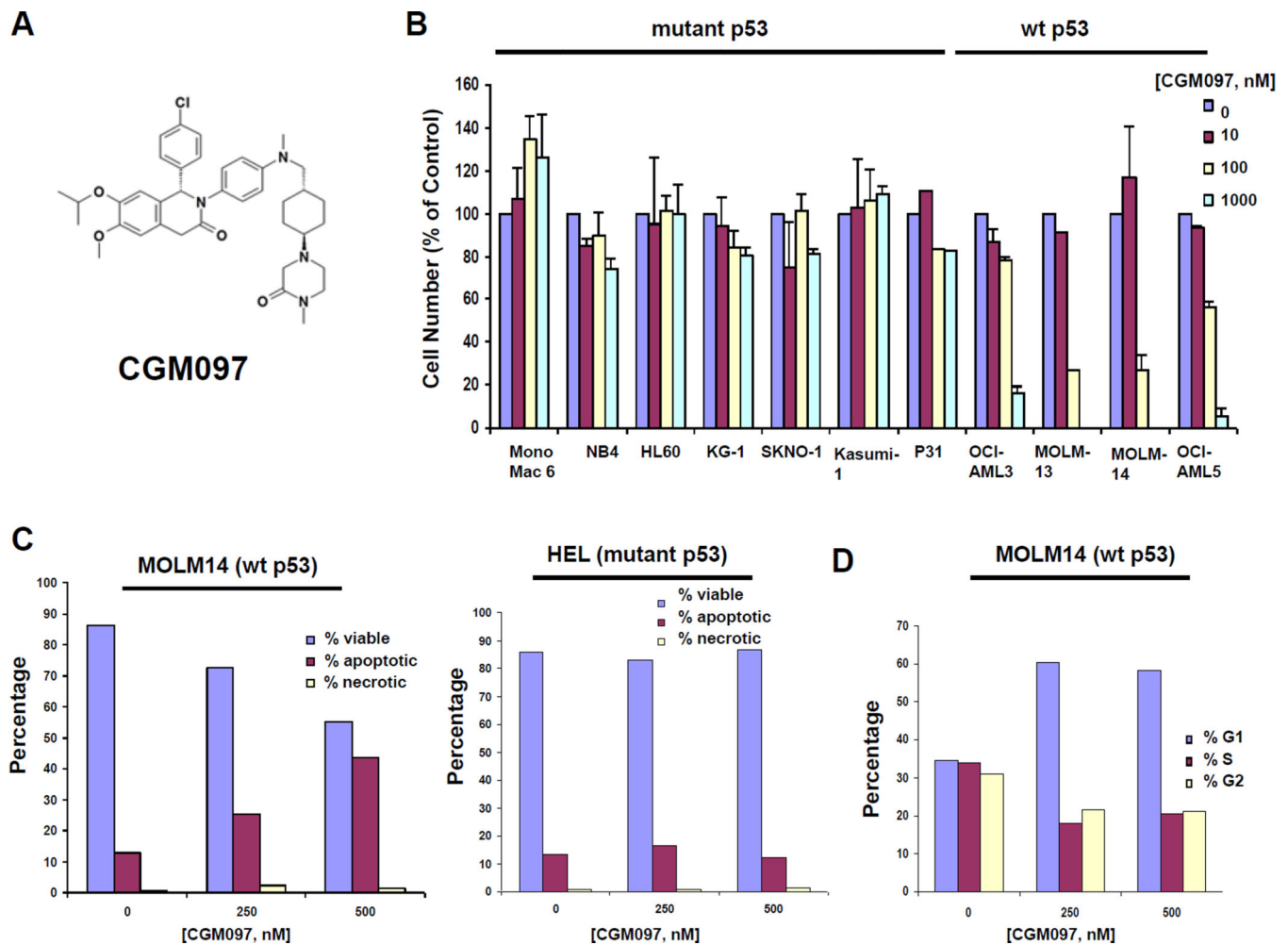


Figure 1. Investigation of CGM097 against human AML cell lines expressing either wt or mutant p53

(A) Chemical structure of CGM097. Effects of CGM097 treatment on proliferation (B), apoptosis (C), and cell cycle progression (D) following approximately three days of treatment. (C–D) Bar graphs are representative of apoptosis and cell cycle data shown in Supplementary Figures 2 and 3, respectively.

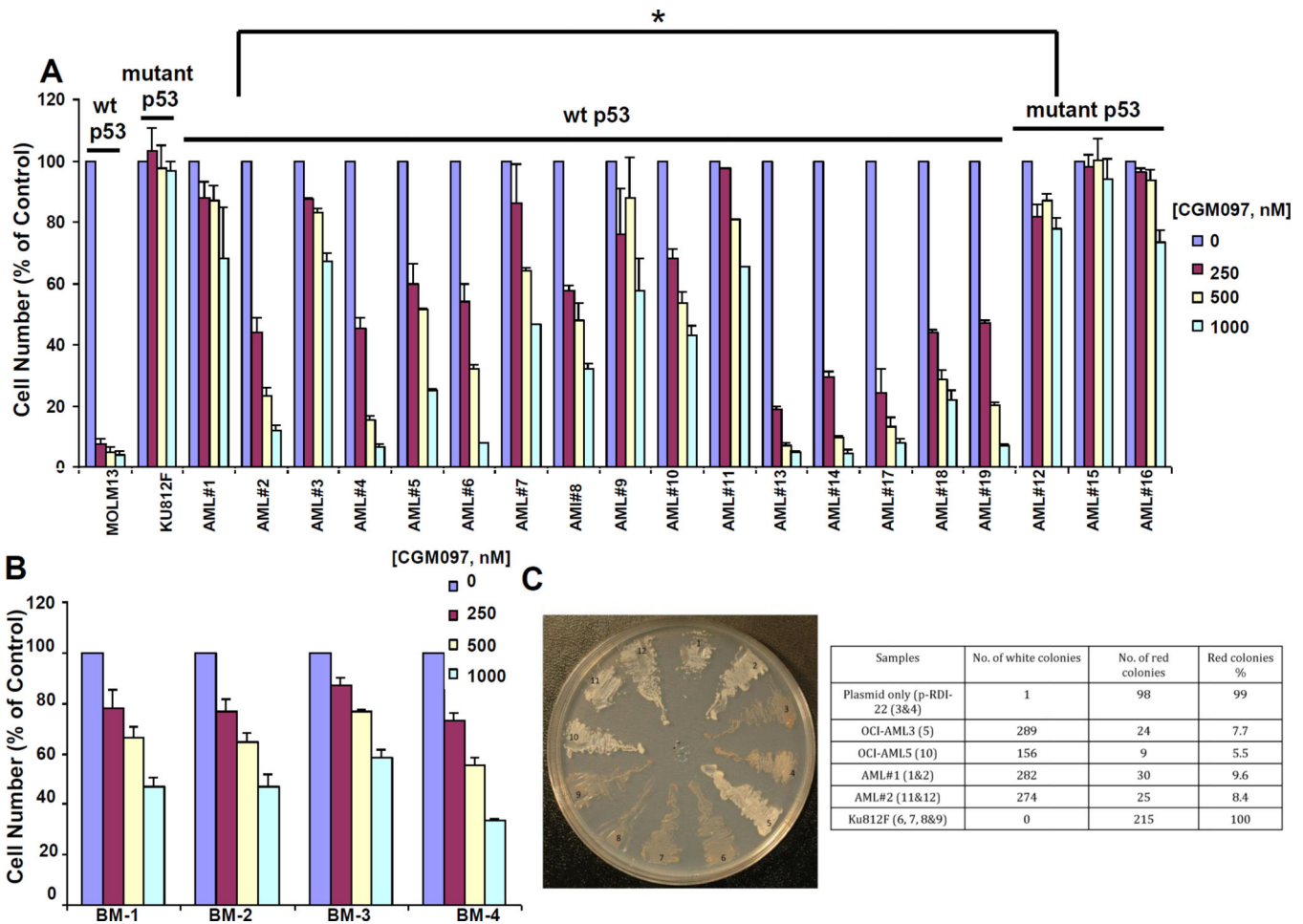


Figure 2. Investigation of CGM097 against primary AML patient cells expressing either wt or mutant p53

CGM097 treatment of primary AML patient samples (A) or normal bone marrow samples (B). MOLM-13 (wt p53-expressing) and KU812F (mutant p53-expressing) are shown as controls for (A) and MOLM14 (wt p53-expressing) is shown as a control for (B). Results shown are following approximately 2–3 days of treatment. Differences in CGM097 responses in wt p53-expressing AML and mutant p53-expressing AML samples were significant as determined by Student's t-test ($p=0.010964621$). (C) Yeast-based p53 functional assay. 1&2: AML patient sample #1 (wt p53); 3&4: pRDI-22 plasmid only; 5: OCI-AML3 (wt p53); 6, 7, 8, & 9: KU812F (mutant p53); 10: OCI-AML5 (wt p53); 11&12: AML patient sample #2 (wt p53).

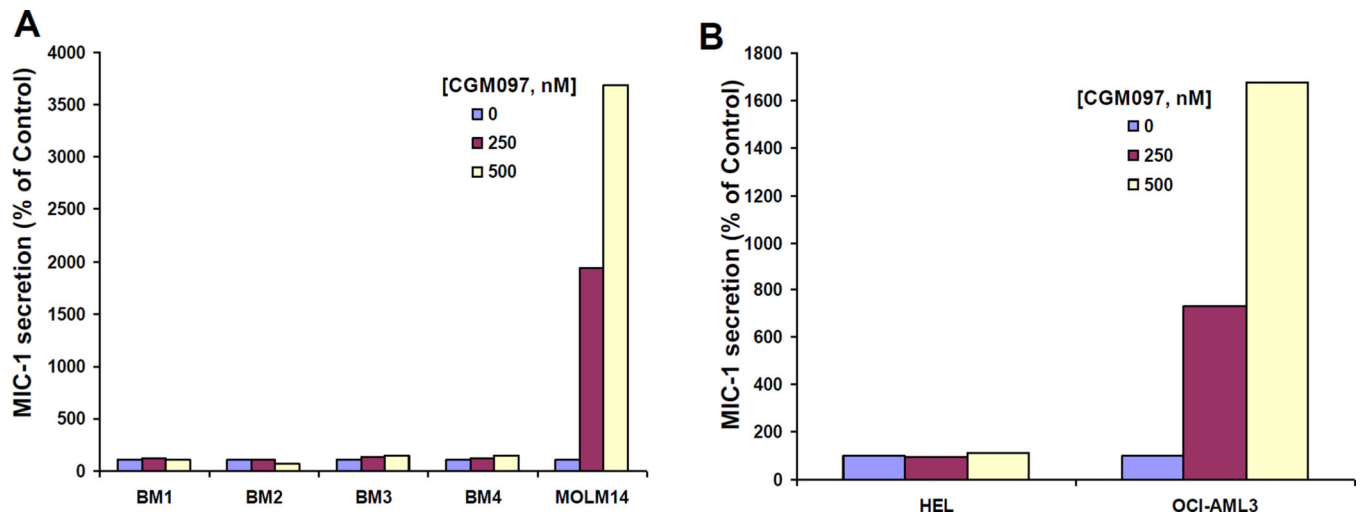


Figure 3. Selective targeting of p53 by CGM097

(A–B) ELISA assay performed with anti-MIC for 15 minutes. Data for each sample were generated using supernatant collected from individual wells of a 24-well plate, with each well representing a single drug concentration.

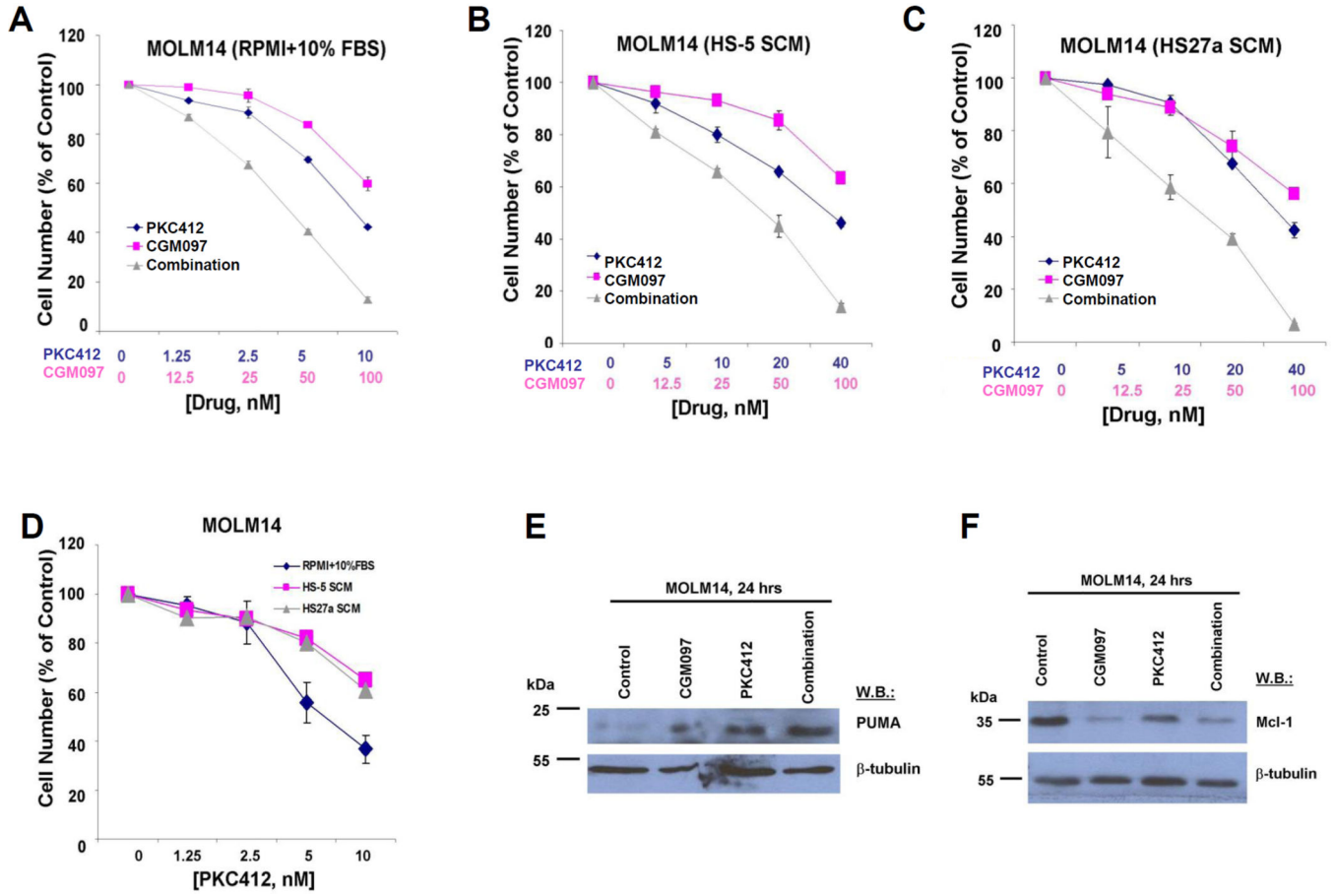


Figure 4. Potentiation of effects of PKC412 or AC220 by CGM097 against mutant FLT3-positive AML cells cultured in the absence and the presence of cytoprotective SCM
 Approximately 2-day treatment of FLT3-ITD-expressing MOLM14 cells with PKC412, CGM097, or a combination of both in the presence of (A) RPMI+10% FBS, (B) HS-5 SCM (90%), (C) HS27a SCM (90%). (D) Direct comparison of effects of PKC412 against MOLM14 cells cultured in the presence of RPMI+10% FBS, HS-5 SCM (90%), or HS27a SCM (90%). (E-F) Investigation of PUMA and Mcl-1 expression in drug-treated MOLM14 cells following 24 hours of treatment.

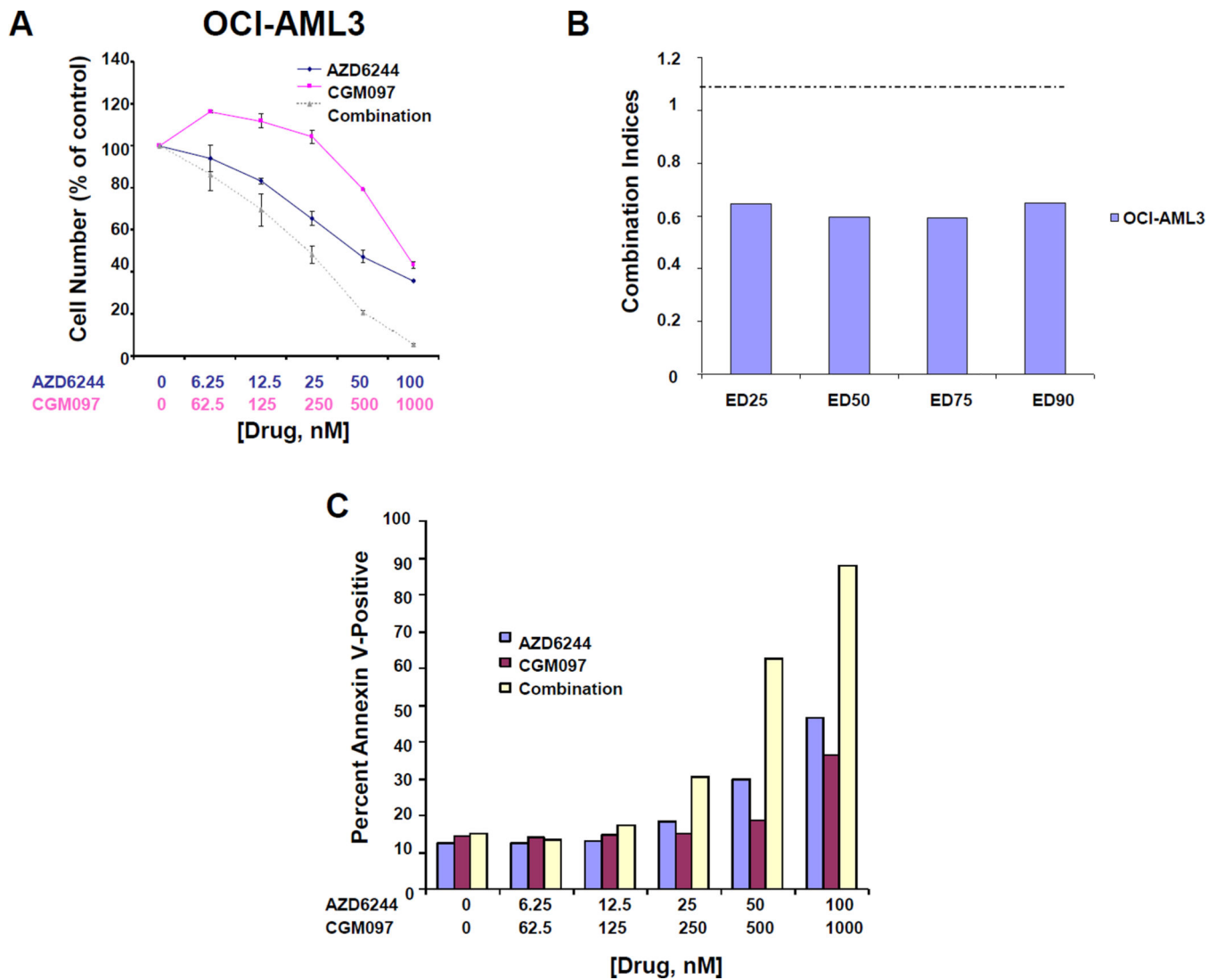


Figure 5. Potentiation of effects of AZD6244 by CGM097 against mutant RAS-positive AML cells

(A) Approximately 3-day treatment of mutant NRAS-expressing OCI-AML3 cells with AZD6244, CGM097, or a combination of both. This study is representative of two independent studies for which similar results were observed. (B) Combination indices calculated for studies in (A). (C) Effects of AZD6244+CGM097 on induction of apoptosis, as compared to either agent alone, against OCI-AML3 cells. Bar graphs shown in “C” are representative of apoptosis data shown in Supplementary Figure 7.

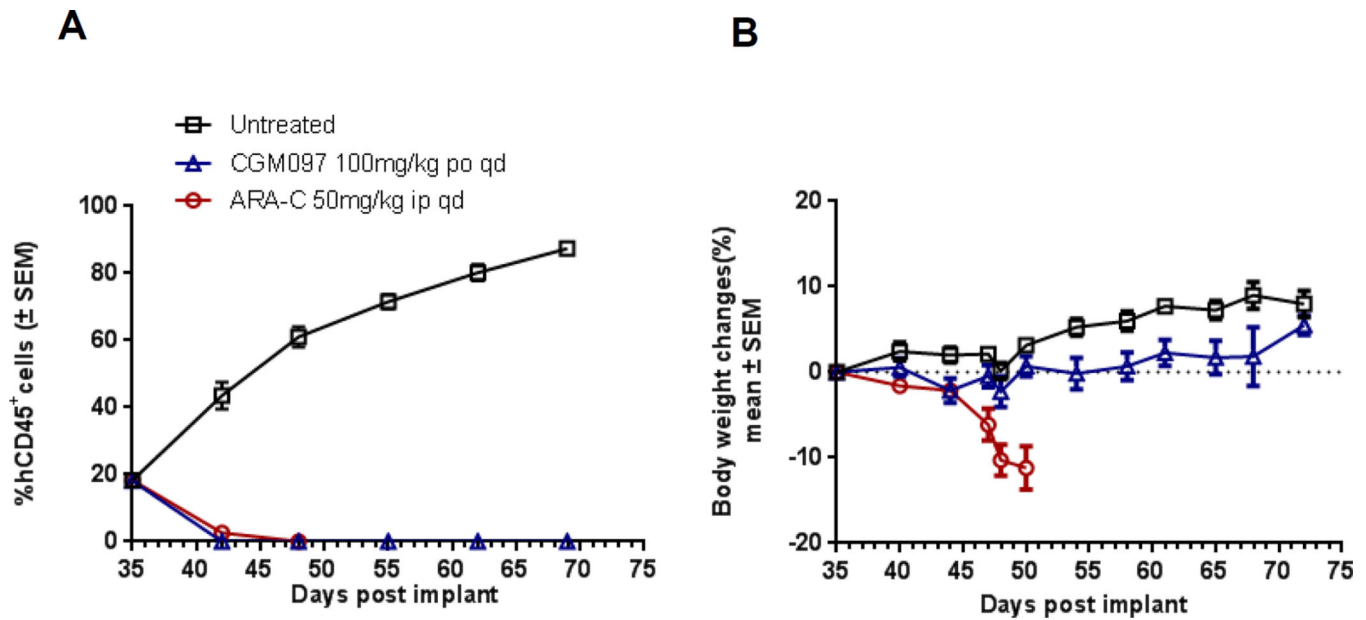


Figure 6. In vivo activity of CGM097 in p53 wt patient-derived AML xenograft

(A) Tumor growth curves of a patient-derived p53 wt AML xenograft treated with CGM097 or ARA-C (standard of care control). Treatment with CGM097 was initiated on day 35 post-implantation, when tumor burden reached 18% (measured by % hCD45+ cells), and continued until day 69 when tumor burden in the untreated group reached 87%.

CGM097 significantly reduced in vivo tumor growth ($P = 0.0004$ by two-tailed unpaired Student's t test). Treatment with ARA-C was initiated on day 35 post implantation, and stopped on day 50 due to body weight loss in all treated mice. Error bars represent S.E.M.

(B) Percent body weight change in mice following treatment. CGM097 dosed at 100mg/kg po qd for 34 days was well-tolerated with no significant body weight changes. ARA-C dosed at 50 mg/kg ip qd for 15 days was not well-tolerated and all mice were sacrificed on day 50 post tumor implantation. Error bars represent S.E.M. AML model details:

HAMLX5340: FLT3-ITD; NPM1 mut; p53WT.

Table I
Combination indices for studies testing the combination of either PKC412+CGM097 or AC220+CGM097 in the presence of RPMI+10% FBS, HS-5 SCM (90%), or HS27a SCM (90%)

All studies are representative of two independent studies for which similar results were observed.

Condition	Combination Indices			
	ED25	ED50	ED75	ED90
RPMI+10% FBS (PKC412+CGM097)	0.78574	0.73627	0.69571	0.66305
HS-5 SCM (PKC412+CGM097)	0.74431	0.63563	0.54300	0.46402
HS27a SCM (PKC412+CGM097)	0.68059	0.60298	0.54904	0.51249
RPMI+10%FBS (AC220+CGM097)	0.80274	0.81577	0.88637	1.03173
HS-5 SCM (AC220+CGM097)	0.70215	0.82179	0.99324	1.24610
HS27a SCM (AC220+CGM097)	0.43172	0.57599	0.77412	1.04741